

# Chladni solitons and the onset of the snaking instability for dark solitons in confined superfluids

A. Muñoz Mateo\* and J. Brand†

Centre for Theoretical Chemistry and Physics and New Zealand Institute for Advanced Study,  
Massey University, Private Bag 102904 NSMC, Auckland 0745, New Zealand

(Dated: November 9, 2018)

Complex solitary waves composed of intersecting vortex lines are predicted in a channeled superfluid. Their shapes in a cylindrical trap include a cross, spoke wheels, and Greek  $\Phi$ , and trace the nodal lines of unstable vibration modes of a planar dark soliton in analogy to Chladni's figures of membrane vibrations. The stationary solitary waves extend a family of solutions that include the previously known solitonic vortex and vortex rings. Their bifurcation points from the dark soliton indicating the onset of new unstable modes of the snaking instability are predicted from scale separation for Bose-Einstein condensates (BECs) and superfluid Fermi gases across the BEC-BCS crossover, and confirmed by full numerical calculations. Chladni solitons could be observed in ultra-cold gas experiments by seeded decay of dark solitons.

PACS numbers: 3.75.Lm,67.85.De,67.85.Lm

Solitons are the hallmark of nonlinear physics. They are ubiquitous in one-dimensional wave propagation and appear in diverse systems ranging from carbon nanotubes [1, 2] and water waves [3] to nonlinear optics [4, 5] and superfluid atomic gases [6–8]. Experimental signatures of vortex rings in trapped BECs [9–11] and the recent observations of solitonic vortices in atomic BECs [12, 13] and a superfluid Fermi gas [8, 14] highlight the richness of solitary wave motion in waveguide-like geometries beyond the one-dimensional paradigm. A solitonic vortex consists of a single vortex line crossing the transverse diameter of an elongated, trapped condensate [15–17], while the vortex line forms a closed loop in a vortex ring. In contrast to vortex lines [18] and rings [19] in bulk superfluids, both structures are heavily influenced by the waveguide trap, leading to localisation with a well-defined step of the superfluid phase across the excitation [15, 20, 21] and modified dynamical properties [14, 22–26]. The systematic numerical study of solitary waves in wave-guide-trapped superfluids has initially been restricted to axisymmetric solitary waves in BECs at weak nonlinearities [17, 20] and has later included the non-axisymmetric solitonic vortex [21]. Here we seek to close the apparent gap and consider complex solitary waves with crossing vortex lines and broken axial symmetry.

Solitary waves probe superfluids at the mesoscopic length scale of the healing length. The physics at these length scales is not very well understood for strongly-correlated superfluids, such as the resonant atomic Fermi gas across the BEC-BCS crossover [27]. In order to provide a reference point for further study, we here employ the recently developed coarse-grained version of the Bogoliubov-de Gennes equation [28] for the crossover superfluid by Simonucci and Strinati [29] at zero temperature, which includes the Gross-Pitaevskii equation in the BEC limit. Previously, the Bogoliubov-de Gennes equations have been used to describe stationary [30] and moving dark solitons [31–34], and the snaking instability [35] in a bulk fermionic superfluid. A variety of other ap-

proaches has also been used to simulate dynamics in the crossover Fermi superfluid [36–39].

The conceptually simplest solitary wave in a superfluid with a scalar, complex order parameter is a stationary kink, or dark soliton, characterised by a node in the order parameter and exponential healing to the background fluid [40] (see also Fig. 1). In two or three dimensions, however, the kink is unstable towards snaking [41] and its stability can only be restored by constricting the geometry to a narrow channel, as e.g. in an elongated atom trap [42]. The appearance of instability modes is connected with the bifurcation of new solitary waves [16]. In this work, we study the complete family of stationary solitary waves bifurcating from the dark soliton in a wave-guide trap geometry. We show that each new solitary wave at the point of bifurcation corresponds to a membrane vibration mode with vortex filaments along its nodal lines. They correspond to the famous Chladni figures that visualise the nodal lines of plate vibrations [43]. We thus call the whole family *Chladni solitons*. Within a scale-separating approximation we derive a simple formula [Eq. (10)] for the bifurcation points in a cylindrically trapped gas in terms of two integer quantum numbers  $p$  and  $l$ , describing the number of vortex rings and radially extending vortex lines, respectively. These results are corroborated by full numerical solutions of the Gross-Pitaevskii equation. We suggest strategies for observing higher order Chladni solitons through the decay of dark solitons.

*Nonlinear Schrödinger model for the BEC-BCS crossover* – In the approach of Simonucci and Strinati [29], the superfluid order parameter  $\Delta(\mathbf{r})$  at zero temperature is determined as the self-consistent solution of a nonlinear Schrödinger equation, which we write as

$$\left[ -\frac{\hbar^2}{4m} \nabla^2 + f(\mu_{\text{loc}}(\mathbf{r}), |\Delta(\mathbf{r})|) \right] \Delta(\mathbf{r}) = 0, \quad (1)$$

where  $m$  is the fermion mass and the local chemical potential  $\mu_{\text{loc}}(\mathbf{r}) = \mu - V(\mathbf{r})$  combines the chemical potential  $\mu$  and the trapping potential  $V(\mathbf{r})$ . The function  $f$  provides

the nonlinearity and can be written as

$$f(\mu, |\Delta|) = -4\mu + 4|\Delta| \frac{I_5}{I_6} - \frac{\pi\hbar\sqrt{|\Delta|}}{\sqrt{2m}a_F I_6}, \quad (2)$$

where  $a_F$  is the  $s$ -wave scattering length of fermions. The functions  $I_5(x_0)$  and  $I_6(x_0)$  are expressed by elliptic integrals and evaluated with the argument  $x_0 = \mu/|\Delta(\mathbf{r})|$  [44]. Equation (1) approximates the Bogoliubov-de Gennes equation [28, 45]. For homogeneous order parameter  $\Delta_0 > 0$ , the resulting equation  $f(\mu, \Delta_0) = 0$  together with the accompanying equation for the density [29] is equivalent to standard BCS theory for the crossover superfluid [45–47]. In the BEC limit  $a_F \rightarrow 0+$ , Eq. (1) reduces to the Gross-Pitaevskii equation [48].

We now proceed to solve Eq. (1) for solitary waves by separation of scales, where the characteristic length scale for the solitary waves  $\xi$  is assumed much smaller than the length scale of order parameter variation due to the presence of the trapping potential  $V(\mathbf{r})$ , on which spatial derivatives can be neglected. This will allow us to understand the solitary waves as excitations on top of a background order parameter  $\Delta_0(\mathbf{r})$ . The latter is obtained using the Thomas Fermi approximation  $f(\mu_{\text{loc}}, \Delta_0) = 0$ , which results from Eq. (1) by neglecting the spatial derivative term. We introduce the length scale  $\xi(\mathbf{r})$  locally, which we expect to be relevant for the solitary waves, by

$$\frac{\hbar^2}{4m\xi^2(\mathbf{r})} = \mu_{\text{loc}}^B(\mathbf{r}) \equiv 2\mu_{\text{loc}}(\mathbf{r}) + \sigma \frac{\hbar^2}{ma_F^2}, \quad (3)$$

where  $\mu_{\text{loc}}^B(\mathbf{r})$  is a local bosonic chemical potential and  $\sigma = 1$  for  $a_F > 0$  and  $\sigma = 0$  otherwise. Rescaling Eq. (1) with this length scale, normalising the order parameter  $\psi(\tilde{\mathbf{r}}) = \Delta(\tilde{\mathbf{r}}\xi)/\Delta_0(\tilde{\mathbf{r}}\xi)$  and ignoring spatial derivatives of the slowly-varying  $\xi(\mathbf{r})$  consistent with the Thomas Fermi approximation, we obtain

$$-\frac{1}{2}\tilde{\nabla}^2\psi - \psi + g(|\psi|^2)\psi = 0, \quad (4)$$

where  $g(|\psi|^2) = 1 + f(\mu_{\text{loc}}, \Delta_0|\psi|)/2\mu_{\text{loc}}^B$ . In units of the background fermion density  $n_0$  with the Fermi wavenumber  $k_F = (3\pi^2 n_0)^{1/3}$  and the Fermi energy  $E_F = \hbar^2 k_F^2/(2m)$  [49], the function  $g$  can be expressed with  $\tilde{\mu} = \mu/E_F$  and the coupling strength  $\eta = 1/(k_F a_F)$  as

$$g(|\psi|^2) = \frac{\sigma\eta^2 + \tilde{\mu} \frac{I_5}{x_0 I_6} - \frac{\eta\pi\sqrt{\tilde{\mu}}}{4\sqrt{x_0} I_6}}{\tilde{\mu} + \sigma\eta^2}, \quad (5)$$

where  $I_5$  and  $I_6$  are evaluated at  $x_0 = x_0^{\text{bg}}/|\psi|$  and  $x_0^{\text{bg}} = \mu_{\text{loc}}/\Delta_0$  is the background value [44]. The dimensionless function  $g$  defines a generalised nonlinearity in the nonlinear Schrödinger equation (4). It weakly depends on position through dependence of  $\eta$  on the background density except in the BEC limit and at unitarity, where it is position independent. While the BEC limit  $\eta \rightarrow +\infty$  [where  $g(|\psi|^2) \rightarrow (1 + |\psi|^2)/2$ ] recovers the cubic nonlinear

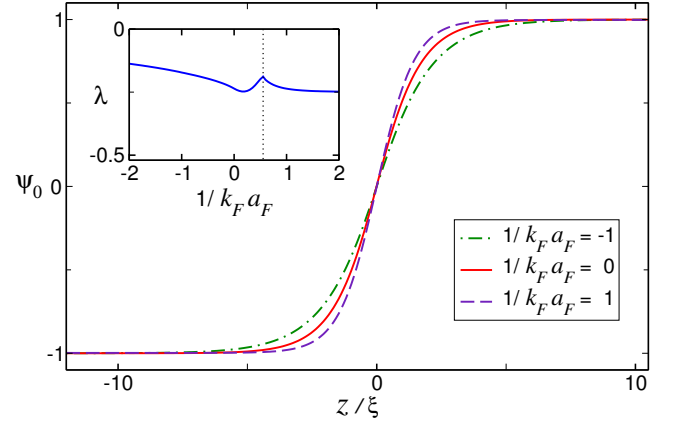


FIG. 1. Superfluid order parameter  $\psi_0(z/\xi)$  of kink solutions of Eq. (4) in the BEC–BCS crossover for different values of the coupling constant  $\eta = 1/k_F a_F$ , where the axial coordinate  $z$  is measured in units of the healing length  $\xi = \hbar/\sqrt{4m\mu^B}$ . The inset shows the (bound) ground state eigenvalue  $\lambda$  of Eq. (6), which modulates the energy available for the excitation of transverse modes. The dotted line indicates the change of sign of the chemical potential.

Schrödinger equation, the function  $g$  simplifies at unitarity ( $\eta = 0$ ) to  $g(|\psi|^2) = I_5/(x_0 I_6)$ , where  $x_0 = x_0^u/|\psi|$  and  $x_0^u \approx 0.8604$  is the background value at unitarity.

*Kink solution and its bifurcations* – The nonlinear Schrödinger equation (4) supports a real kink solution  $\psi_0(\tilde{\mathbf{r}})$  that depends on  $\tilde{z}$  only with a single node at  $\tilde{z} = 0$  and boundary condition  $\psi_0 \rightarrow \pm 1$  as  $\tilde{z} \rightarrow \pm\infty$ , respectively, as shown in Fig. 1. Bifurcations of symmetry breaking solutions are found by using the ansatz  $\psi = \psi_0 + i\delta\psi$  and linearising Eq. (4) for a completely imaginary perturbation  $i\delta\psi$ . Due to the symmetry of the original kink solution  $\psi_0$ , the perturbation can further be separated with the product ansatz  $\delta\psi = \chi(\tilde{x}\xi, \tilde{y}\xi)u(\tilde{z})$ . For  $u$  this yields the eigenvalue equation

$$\left[ -\frac{1}{2}\partial_{\tilde{z}\tilde{z}} - 1 + g(|\psi_0(\tilde{z})|^2) \right] u = \lambda u. \quad (6)$$

This Schrödinger equation with localised potential well has a one-node solution  $u = \psi_0$ , which corresponds to the Goldstone mode of phase symmetry with  $\lambda = 0$ . More relevant for bifurcating solitary waves, Eq. (6) has a nodeless and localised solution with eigenvalue  $\lambda < 0$ . In the BEC limit,  $1 - g(|\psi_0|^2) = \text{sech}^2(\tilde{z}/\sqrt{2})/2$  is a Rosen-Morse potential with analytically known solution  $u = \text{sech}(\tilde{z}/\sqrt{2})$  and eigenvalue  $\lambda = -1/4$  [50]. For finite values of the coupling constant  $\eta$ ,  $\lambda$  can be determined numerically and is shown in the inset of Fig. 1. At unitarity, we obtain  $\lambda = -0.24$ .

For the transverse wave function  $\chi$  we obtain by restoring the unscaled coordinates the wave equation

$$\left[ -\frac{\xi^2}{2}\nabla_{\perp}^2 + \lambda \right] \chi = 0. \quad (7)$$

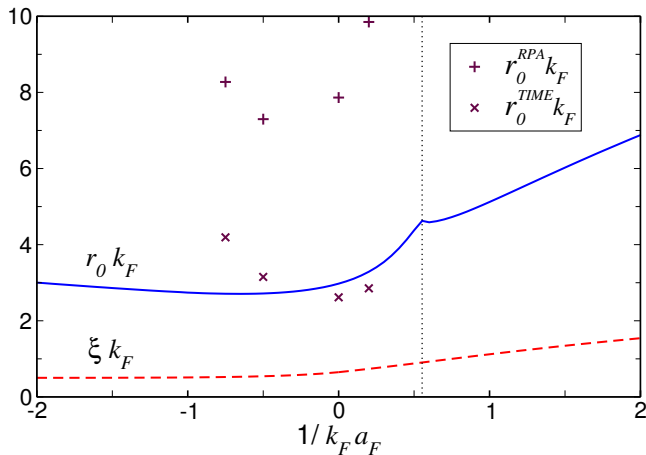


FIG. 2. Length scale  $r_0$  (full line) of the snaking instability given by Eq. (8) and healing length  $\xi$  of Eq. (3) (dashed line) as functions of the interaction parameter  $1/k_F a_F$  of the BEC–BCS crossover. For comparison, the results from time-dependent Bogoliubov-de Gennes simulations and RPA of Ref. [35] are shown.

In the absence of a trapping potential,  $\xi$  is constant. The real-valued solutions are readily found as standing waves with nodal lines separated by a distance

$$r_0 = \frac{\pi}{\sqrt{-2\lambda}} \xi, \quad (8)$$

which is the minimum length scale of the snaking instability [16]. In Fig. 2 the value of  $r_0$  is compared with the numerical results of Ref. [35], which suffered inaccuracies due to numerical limitations for grid size and cutoff parameters.

In the presence of a trapping potential, the influence of the snaking instability can be made explicit in rewriting Eq. (7) as

$$\left\{ -\frac{\hbar^2}{4m} \nabla_{\perp}^2 - \lambda [4V(\mathbf{r}) - 2\mu^B] \right\} \chi = 0. \quad (9)$$

This is a two-dimensional Schrödinger equation with a scaled external potential and prescribed eigenvalue. For the case of harmonic isotropic trapping with  $V(\mathbf{r}) = \frac{1}{2}m\omega_{\perp}^2(x^2 + y^2)$  we obtain the condition for the bifurcation points

$$\frac{\mu^B}{\hbar\omega_{\perp}} = \frac{2p + l + 1}{\sqrt{-2\lambda}}, \quad (10)$$

where  $p$  and  $l$  are the radial and azimuthal quantum numbers of the cylindrical harmonic oscillator eigenfunctions  $|p, l\rangle \propto \exp(-r_{\perp}^2/2a_{\perp}^2)r_{\perp}^l L_p^l(r_{\perp}^2/a_{\perp}^2) \cos(l\theta)$ , and  $L_p^l$  are the associated Laguerre polynomials in  $r_{\perp}^2 = x^2 + y^2$ , with the characteristic oscillator length  $a_{\perp} = \sqrt{\hbar/m\omega_{\perp}}$ . The condition (10) together with the harmonic oscillator eigenfunctions defines the bifurcation points as well as the shape, symmetry, and degeneracy of the corresponding bifurcating vortex solutions.

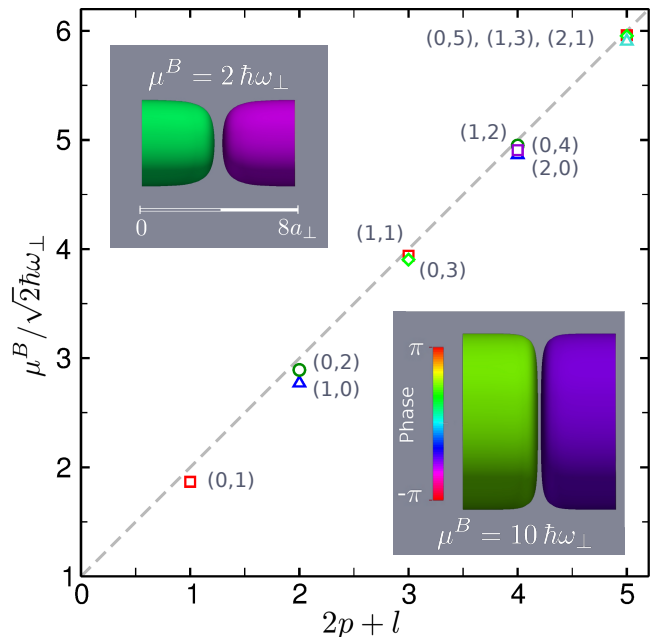


FIG. 3. Bifurcation points for the emergence of Chladni solitons with quantum numbers  $(p, l)$  from the planar kink in a cylindrically confined BEC. Numerical data (labeled open symbols) obtained from solving the Gross-Pitaevskii equation are compared with the analytical prediction (dashed line) of Eq. (10) with  $\lambda = -\frac{1}{4}$ . The insets display 3D density isocontours of dark soliton states at 5% of maximum density in the weak (upper left) and strong (lower right) nonlinearity regimes.

Numerical data for the bifurcation points in the BEC limit are shown in Fig. 3. The agreement with Eq. (10) is surprisingly good even for small quantum numbers. The first bifurcation point corresponds to a single straight nodal line ( $p = 0, l = 1$ ) and leads to the solitonic vortex (SV), shown in the central inset of Fig. 4. It marks the onset of the snaking instability for the kink. Its accurate numerical value of  $\mu^B/\hbar\omega_{\perp} = 2.65$  is very close to the value  $2\sqrt{2} \approx 2.82$  of Eq. (10) and consistent with Ref. [17]. The next bifurcation point comes from the degenerate solutions  $(1, 0)$  and  $(0, 2)$ , corresponding to a single vortex ring (VR) originating from a radial node and to two crossed solitonic vortices (2SV) originating from two azimuthal nodes, respectively. Our numerical results resolve the degeneracy breaking between the VR ( $\mu^B/\hbar\omega_{\perp} = 3.9$ ) and 2SV (4.1) bifurcation points (see Fig. 3) that cannot be captured by our analytical model ( $3\sqrt{2} \approx 4.2$ ). Similar degeneracy breaking occurs for higher quantum numbers  $(p, l)$ . Overall, the agreement with the analytic result of Eq. (10) improves for higher quantum numbers corresponding to larger  $\mu$ . This is expected since the underlying approximation – scale separation between Thomas Fermi radius and healing length – is increasingly satisfied.

In the more general case of an anisotropic transverse trapping potential  $V(\mathbf{r}) = \frac{1}{2}m(\omega_x^2 x^2 + \omega_y^2 y^2)$  the bi-

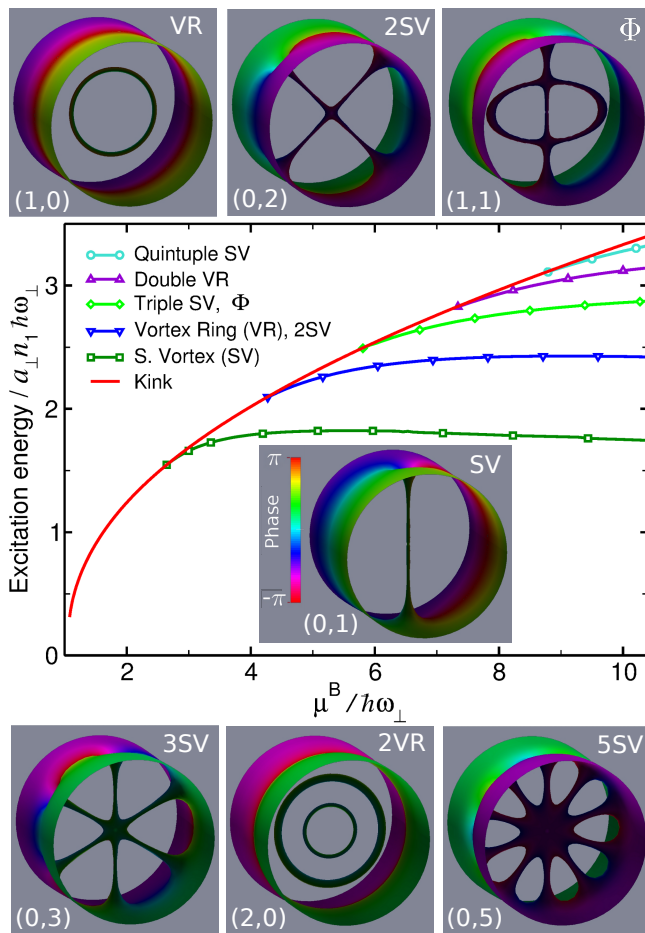


FIG. 4. Free excitation energy  $F_{pl}$  of stationary solitary waves vs. chemical potential in a cylindrically trapped BEC (central panel). The full (red) line corresponds to the dark soliton [see insets in Fig. (3)] and lines with symbols correspond to Chladni solitons  $(p, l)$  originated from the bifurcation points of Fig. 3. Units of the transverse harmonic trap and axial density  $n_1$  are used as shown. The insets show density isocontours at 5% of maximum density for the different Chladni solitons with  $\mu^B = 10\hbar\omega_\perp$ .

furcation condition (10) is modified to read  $\mu^B \sqrt{-2\lambda} = (n_x + \frac{1}{2})\hbar\omega_x + (n_y + \frac{1}{2})\hbar\omega_y$ . The corresponding harmonic oscillator eigenfunctions are given by the well known Hermite functions and thus the symmetry of the corresponding Chladni solitons changes. For small anisotropies, we expect a continuous transition from Laguerre to Hermite shapes as is shown by Ince polynomials [51].

*Chladni solitons* – We have numerically determined the solitary wave solutions originating from the bifurcation points of Fig. 3 up to  $\mu^B = 10\hbar\omega_\perp$  using a Newton-Raphson scheme for the Gross-Pitaevskii equation. The results are summarised in Fig. 4, where the free excitation energies  $F_{pl} = E_{pl} - \mu^B N_{pl} - (E_0 - \mu^B N_0)$  are measured relative to the ground state  $\phi_0$  of Eq. (11) [52]. For every tuple of quantum numbers  $(p, l)$  we obtain solitary wave solutions with symmetry and degeneracy consistent with

the solutions of Eq. (9), which is maintained for  $\mu^B$  above the bifurcation point. I.e. Chladni solitons involving vortex rings have a discrete 2-fold degeneracy while all solitons involving radial vortex lines have a continuous degeneracy corresponding to azimuthal rotation.

In addition to the previously known dark soliton (kink), solitonic vortex  $(0, 1)$ , and vortex ring  $(2, 0)$ , more complex Chladni solitons comprise *spoke wheels*  $(0, l)$  consisting of  $l > 1$  intersecting radial vortex lines, multiple nested vortex rings  $(p, 0)$  and the  $\Phi$ -type soliton  $(1, 1)$ , which is the simplest soliton with intersecting vortex ring(s) and radial line(s). Note that Chladni solitons originating from near-degenerate bifurcation points, e.g. the 2SV cross  $(0, 2)$  and vortex ring  $(1, 0)$  are almost degenerate also for larger  $\mu^B$  and their small energy difference is not resolved at the scale of Fig. 4. The same is true for the higher near-degenerate branches.

Our numerical simulations indicate that Chladni solitons with intersecting vortex lines could be observed in cigar-shaped BECs. Although the solitonic vortex  $(0, 1)$  is the only dynamically stable Chladni soliton for  $\mu^B$  beyond the first bifurcation point of Eq. (10), the expected lifetimes of the  $2p + l > 1$  Chladni solitons are comparable to those of the already observed vortex rings. Detailed stability studies will be published elsewhere [53]. Complex Chladni solitons can be prepared in an atomic BEC by appropriately seeding the snaking instability of a dark soliton. For this purpose, the previously determined wave function  $\psi = \psi_0 + i\delta\psi$  at the bifurcation point, should be an excellent initial configuration, since the infinitesimal part  $\delta\psi$  develops into a dynamically unstable mode leading to the desired complex soliton for  $\mu^B$  larger than the critical value at bifurcation [16]. As a first step we propose to prepare a zero velocity dark-bright soliton in a two-component BEC [54] as in Refs. [9, 55], where the nodal plane of a kink in component  $|1\rangle$  is filled with a phase-coherent atomic BEC of a second hyperfine component  $|2\rangle$ . In a second step, the bright component  $|2\rangle$  (or a small part of it) is transferred to state  $|1\rangle$  with the appropriate phase pattern of the solution  $\delta\psi = \chi u$  of Eqs. (6) and (9), shifted by  $\frac{\pi}{2}$  compared to the kink solution. This could be realised following [56] by transferring the phase pattern of a focused axial Laguerre-Gaussian laser beam using a two-photon Raman transition. Finally, any remaining  $|2\rangle$  atoms are removed [9].

*Acknowledgements* – We are grateful to Michael Bromley and Xiaoquan Yu for useful discussions.

\* A.M.Mateo@massey.ac.nz

† J.Brand@massey.ac.nz

- [1] C. Chamon, Phys. Rev. B **62**, 2806 (2000).
- [2] V. V. Deshpande and M. Bockrath, Nat. Phys. **4**, 314 (2008).
- [3] A. Chabchoub, O. Kimmoun, H. Branger, N. Hoffmann, D. Proment, M. Onorato, and N. Akhmediev, Phys. Rev. Lett. **110**, 124101 (2013).

- [4] Y. S. Kivshar and B. Luther-Davies, *Phys. Rep.* **298**, 81 (1998).
- [5] A. Amo, S. Pigeon, D. Sanvitto, V. G. Sala, R. Hivet, I. Carusotto, F. Pisanello, G. Leménager, R. Houdré, E. Giacobino, C. Ciuti, and A. Bramati, *Science* **332**, 1167 (2011).
- [6] S. Burger, K. Bongs, S. Dettmer, W. Ertmer, and K. Sengstock, *Phys. Rev. Lett.* **83**, 5198 (1999).
- [7] J. Denschlag, J. E. Simsarian, D. L. Feder, C. W. Clark, L. A. Collins, J. Cubizolles, L. Deng, E. W. Hagley, K. Helmerson, W. P. Reinhardt, S. L. Rolston, B. I. Schneider, and W. D. Phillips, *Science* **287**, 97 (2000).
- [8] T. Yefsah, A. T. Sommer, M. J. H. Ku, L. W. Cheuk, W. Ji, W. S. Bakr, and M. W. Zwierlein, *Nature* **499**, 426 (2013).
- [9] B. P. Anderson, P. C. Haljan, C. A. Regal, D. L. Feder, L. A. Collins, C. W. Clark, and E. A. Cornell, *Phys. Rev. Lett.* **86**, 2926 (2001).
- [10] Z. Dutton, M. Budde, C. Slowe, and L. V. Hau, *Science* **293**, 663 (2001).
- [11] N. Ginsberg, J. Brand, and L. Hau, *Phys. Rev. Lett.* **94**, 40403 (2005).
- [12] C. Becker, K. Sengstock, P. Schmelcher, P. G. Kevrekidis, and R. Carretero-González, *New J. Phys.* **15**, 113028 (2013).
- [13] S. Donadello, S. Serafini, M. Tylutki, L. P. Pitaevskii, F. Dalfovo, G. Lamporesi, and G. Ferrari, *Phys. Rev. Lett.* **113**, 065302 (2014).
- [14] M. J. H. Ku, W. Ji, B. Mukherjee, E. Guardado-Sanchez, L. W. Cheuk, T. Yefsah, and M. W. Zwierlein, *Phys. Rev. Lett.* **113**, 065301 (2014).
- [15] J. Brand and W. P. Reinhardt, *J. Phys. B At. Mol. Opt. Phys.* **34**, L113 (2001).
- [16] J. Brand and W. Reinhardt, *Phys. Rev. A* **65**, 043612 (2002).
- [17] S. Komineas and N. Papanicolaou, *Phys. Rev. A* **68**, 043617 (2003).
- [18] L. Pitaevskii and S. Stringari, *Bose-Einstein Condensation* (Clarendon, Oxford, 2003).
- [19] C. A. Jones and P. H. Roberts, *J. Phys. A. Math. Gen.* **15**, 2599 (1982).
- [20] S. Komineas and N. Papanicolaou, *Phys. Rev. Lett.* **89**, 070402 (2002).
- [21] S. Komineas and N. Papanicolaou, *Phys. Rev. A* **67**, 023615 (2003).
- [22] A. L. Fetter and A. A. Svidzinsky, *J. Phys. Condens. Matter* **13**, R135 (2001).
- [23] T.-L. Horng, S.-C. Gou, and T.-C. Lin, *Phys. Rev. A* **74**, 041603 (2006).
- [24] C.-H. Hsueh, S.-C. Gou, T.-L. Horng, and Y.-M. Kao, *J. Phys. B At. Mol. Opt. Phys.* **40**, 4561 (2007).
- [25] L. P. Pitaevskii, (2013), arXiv:1311.4693.
- [26] A. Bulgac and M. M. Forbes, (2013), arXiv:1312.2563.
- [27] S. Giorgini and S. Stringari, *Rev. Mod. Phys.* **80**, 1215 (2008).
- [28] P. G. D. Gennes, *Superconductivity Of Metals And Alloys* (Westview Press, 1999).
- [29] S. Simonucci and G. C. Strinati, *Phys. Rev. B* **89**, 054511 (2014).
- [30] M. Antezza, F. Dalfovo, L. Pitaevskii, and S. Stringari, *Phys. Rev. A* **76**, 043610 (2007).
- [31] R. Scott, F. Dalfovo, L. Pitaevskii, and S. Stringari, *Phys. Rev. Lett.* **106**, 185301 (2011).
- [32] A. Spuntarelli, L. D. Carr, P. Pieri, and G. C. Strinati, *New J. Phys.* **13**, 035010 (2011).
- [33] R. Liao and J. Brand, *Phys. Rev. A* **83**, 041604(R) (2011).
- [34] R. G. Scott, F. Dalfovo, L. P. Pitaevskii, S. Stringari, O. Fialko, R. Liao, and J. Brand, *New J. Phys.* **14**, 023044 (2012).
- [35] A. Cetoli, J. Brand, R. G. Scott, F. Dalfovo, and L. P. Pitaevskii, *Phys. Rev. A* **88**, 043639 (2013).
- [36] A. Bulgac, Y.-L. Luo, P. Magierski, K. J. Roche, and Y. Yu, *Science* **332**, 1288 (2011).
- [37] G. Wlazowski, A. Bulgac, M. M. Forbes, and K. J. Roche, (2014), arXiv:1404.1038.
- [38] W. Wen, C. Zhao, and X. Ma, *Phys. Rev. A* **88**, 063621 (2013).
- [39] P. Scherpelz, K. Padavić, A. Rançon, A. Glatz, I. S. Aranson, and K. Levin, (2014), arXiv:1401.8267.
- [40] T. Tsuzuki, *J. Low Temp. Phys.* **4**, 441 (1971).
- [41] E. Kuznetsov and S. Turitsyn, *Sov. Phys. JETP* **67**, 1583 (1988).
- [42] A. E. Muryshev, H. B. van Linden van den Heuvell, and G. V. Shlyapnikov, *Phys. Rev. A* **60**, R2665 (1999).
- [43] E. F. F. Chladni, *Entdeckungen über die Theorie des Klanges* (Weidmanns Erben und Reich, 1787).
- [44] In terms of the complete elliptic integrals of the first and second kind  $K(\kappa)$  and  $E(\kappa)$ , respectively,  $I_5(x_0) = (1 + x_0^2)^{1/4}E(\kappa) - K(\kappa)/[4x_1^2(1 + x_0^2)^{1/4}]$  and  $I_6(x_0) = K(\kappa)/[2(1 + x_0^2)^{1/4}]$ , with  $x_1^2 = (\sqrt{1 + x_0^2} + x_0)/2$  and  $\kappa^2 = x_1^2/\sqrt{1 + x_0^2}$  [29, 47]. We use notation for elliptic integrals conforming with [57].
- [45] A. J. Leggett, in *Mod. Trends Theory Condens. Matter*, Lecture Notes in Physics, edited by A. Pkalski and J. Przystawa (Springer Berlin Heidelberg, 1980) pp. 13–27.
- [46] D. Eagles, *Phys. Rev.* **186**, 456 (1969).
- [47] M. Marini, F. Pistolesi, and G. Strinati, *Eur. Phys. J. B* **1**, 151 (1998).
- [48] For large and positive  $1/(k_F a_F) \gg 1$  (BEC limit), Eq. (1) reduces to the Gross-Pitaevskii equation
- $$\left[ -\frac{\hbar^2}{2m_B} \nabla^2 - \mu^B + V_B(\mathbf{r}) + g_B |\phi|^2 \right] \phi(\mathbf{r}) = 0, \quad (11)$$
- where  $m_B = 2m$  is the mass of bosons,  $V_B = 2V$ ,  $\mu^B = 2\mu + \hbar^2/(ma_F^2)$  is the boson chemical potential,  $\phi(\mathbf{r}) = \Delta(\mathbf{r})\sqrt{\frac{m^2 a_F}{8\pi\hbar^4}}$  the Gross-Pitaevskii order parameter, and  $g_B = 4\pi\hbar^2 a_B/m_B$  the coupling strength [29].
- [49] The background density  $n_0$  used here to define the unit system is related to the chemical potential  $\mu_{\text{loc}}^B$  and  $a_F$  by the standard relations of crossover BCS theory [29]. It depends on position weakly, i.e. its spatial derivatives are ignored.
- [50] N. Rosen and P. M. Morse, *Phys. Rev.* **42**, 210 (1932).
- [51] M. A. Bandres and J. C. Gutiérrez-Vega, *J. Opt. Soc. Am. A* **21**, 873 (2004).
- [52] We use the standard expressions for energy
- $$E = \int d\mathbf{r} \left\{ \frac{\hbar^2}{2m_B} |\nabla\phi|^2 + V_B |\phi|^2 + \frac{g_B}{2} |\phi|^4 \right\}, \quad (12)$$
- and particle number  $N = \int d\mathbf{r} n$ , consistent with the Gross-Pitaevskii equation [48], where  $n(\mathbf{r}) = |\phi(\mathbf{r})|^2$ .
- [53] A. Muñoz Mateo and J. Brand, in preparation (2014).
- [54] T. Busch and J. Anglin, *Phys. Rev. Lett.* **87**, 010401 (2001).
- [55] C. Becker, S. Stellmer, P. Soltan-Panahi, S. Dörscher, M. Baumert, E.-m. Richter, J. Kronjäger, K. Bongs, and K. Sengstock, *Nat. Phys.* **4**, 496 (2008).

- [56] R. Dum, J. Cirac, M. Lewenstein, and P. Zoller, *Phys. Rev. Lett.* **80**, 2972 (1998).
- [57] F. W. J. Olver, D. W. Lozier, R. F. Boisvert, and C. W. Clark,

eds., *NIST Handbook of Mathematical Functions* (Cambridge University Press, 2010).